International Agrophysics 5 (3–4), pp. 171–181 (1989)

CLIMATE AND THE EARTH'S RADIATION BUDGET

A NASA multisatellite experiment has determined that clouds cool the planet more than they heat it and identified them as a major source of uncertainty in three-dimensional models used for studying the greenhouse effect and global warming.

V. Ramanathan, Bruce R. Barkstrom and Edwin F. Harrison

Among the first payloads aboard satellites in the early 1960s were instruments for measuring the Earth's radiation budget.[1] The radiation budget consists of the incident and reflected sunlight and the long-wave (infrared and far infrared) radiation emitted to space. The source for the recent spurt in scientific and public interest in the greenhouse effect and global warming is the alteration of the radiation budget by the anthropogenic emission of trace gases into the atmosphere.

After two decades of progress in satellite instrumentation, the Earth Radiation Budget Experiment[2] began in the 1980s. ERBE instruments are carried on three satellites: the Earth Radiation Budget Satellite, NOAA-9 and NOAA-10. The instruments on ERBS (launched by the space shuttle Challenger) began observing the Earth in November 1984; those on NOAA-9, in February 1985; and those on NOAA-10, in December 1986. These instruments are still collecting data critical to understanding the greenhouse effect. The data are also fundamental to defining the role of human activities in climate change.

Global radiation energy balance

To understand more fully the role of these satellites and to appreciate the implications of their observations of the radiation budget for theories of climate, it is useful to examine a few simple, conceptual models of climate. Such models illustrate the strong links among the radiation budget, the climate and the circulation of the atmosphere and the oceans. As we shall see, the effects of cloud cover may be the greatest sources of uncertainty in our understanding of climate and how it responds to human activities.[3]

The simplest zero-dimensional model of climate considers the long-term average (on a time scale greater than a year) of the global and annual mean temperature. A balance between the absorbed solar energy and the emitted energy governs this temperature. We can write this symbolically as

$$H = \frac{S_0}{4}(1 - \alpha) - \sigma T_e^4 = 0$$

Here H is the net energy input to the climate system. The solar irradiance S_0 is the solar power per unit area intercepted at the mean Earth–Sun distance; recent satellite measurements show that S_0 is about 1365–1372 W/m^2. In the equation, the geometric factor 4 is the ratio of the Earth's surface area to the area of the Earth's disk. The planetary albedo α is the fraction of the solar irradiance reflected by the planet's surface and atmosphere; past satellite measurements show that α is 0.30 ± 0.03. The surface–atmosphere system is assumed to emit like a blackbody at a temperature T_e. (The coefficient σ is the Stefan–Boltzmann constant.) Although the surface emission is close to that of a blackbody, the atmosphere emits in specific wavelength bands, and so the emission departs significantly from that of a blackbody. T_e is still a useful parameter, however, provided we think of it as a planet's *effective* radiating temperature. Thus, we expect T_e to be 255 K if H is zero.

What does this effective radiating temperature, T_e, mean? If the atmosphere did not impede the radiative energy flow, the surface temperature T_s would be nearly the same as T_e. T_s, however, is observed to be 288 K. The 33-K difference is attributed to the greenhouse effect.

Satellite measurements of the radiation budget show

V. Ramanathan is a professor in the department of geophysical sciences at the University of Chicago. **Bruce R. Barkstrom**, science team leader of the Earth Radiation Budget Experiment, is a senior scientist in the atmospheric sciences division of NASA's Langley Research Center, Hampton, Virginia. **Edwin F. Harrison** is a senior scientist and head of the radiation sciences branch in the same division.

Akadémiai Kiadó/Agroinform, Budapest
Kluwer Academic Publishers

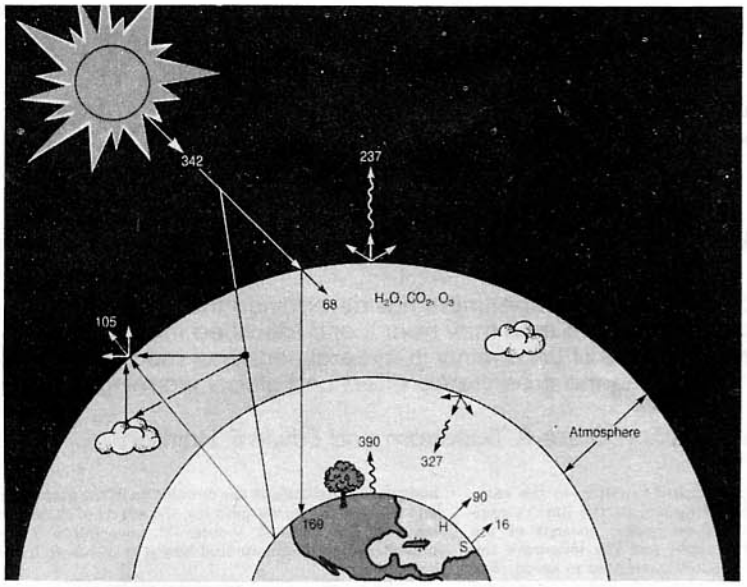

Global energy balance for annual mean conditions. For the top of the atmosphere, the estimates of solar insolation (342 W/m²), reflected solar radiation (105 W/m²) and outgoing long-wave radiation (237 W/m²) are obtained from satellite data. The other quantities are obtained from various published model and empirical estimates. These quantities include atmospheric absorption of solar radiation (68 W/m²); surface absorption of solar radiation (169 W/m²); downward long-wave emission by the atmosphere (327 W/m²); upward long-wave emission by the surface (390 W/m²); *H*, the latent heat flux from the surface (90 W/m²); and *S*, the turbulent heat flux from the surface (16 W/m²). *H* and *S* are averaged over both ocean and land. **Figure 1**

this difference more directly. Let us make an illustrative calculation based on the numbers in figure 1. At a temperature of 288 K, the surface emits 390 W/m². Only 237 W/m² escapes to space. The energy trapped in the atmosphere is the 153 W/m² difference between the surface emission and the total energy loss.

Because the atmosphere is generally colder than the ground, we know from the blackbody radiation law that a molecule in the atmosphere will absorb more energy than it emits. The net result of these absorption and emission processes is that part of the infrared radiation emitted by the ground is trapped. The infrared trapping by the atmosphere—familiarly known as the greenhouse effect—is due primarily to water vapor, clouds and CO_2, with a smaller, 5% contribution from the gases O_3, N_2O and CH_4. But several anthropogenic gases, however, such as the chlorofluorocarbons like $CFCl_3$ and CF_2Cl_2, are now beginning to make an appreciable contribution.

Radiative–convective equilibrium

Now let us turn to a one-dimensional model rather than a zero-dimensional model. The atmosphere constantly loses energy (see figure 1) because it emits 327 W/m² to the surface. The atmosphere traps 153 W/m² of long-wave radiation (as we showed before) and absorbs only 68 W/m² from the Sun. Hence the atmosphere loses 106 (that is, $-327 + 153 + 68$) W/m² of radiation energy. In other words, there is radiative cooling of the atmosphere and a corresponding radiative heating of the Earth's surface. (The surface must gain 106 W/m² to balance the 106 W/m² atmospheric loss.)

Heating the lower boundary of a fluid while cooling its interior is the classical mechanism for inducing convective instability and turbulence. In the Earth's atmosphere, evaporation of water from the surface and condensation elsewhere complicates the heat exchange. Turbulent transfer of heat and condensation of water make up for the atmosphere's radiative energy deficit (see figure 2). The combination of these nonradiative processes is loosely called convective heat transport.

The convective stirring of the atmosphere is so efficient that it drives the atmosphere toward a neutral thermal lapse rate ($-dT/dZ$, or the negative change in temperature with height). The troposphere is defined as the region in which nonradiative processes govern the lapse rate; the stratosphere is the region in which the radiative-equilibrium lapse rate agrees with the observed lapse rate. The boundary between these two regions is the tropopause. Once the lapse rate is prescribed, the surface temperature is the only degree of freedom for the troposphere; it is determined by the net (down minus up) flux of the solar and infrared radiation at the tropopause.

The radiation fluxes at the upper boundary are influenced strongly by internal parameters such as the

distribution of water vapor, clouds and other gases; by the lapse rate; and by surface properties such as ice and snow cover, vegetation types and soil moisture. The dependence of these parameters on the surface temperature T_s gives rise to several feedback loops, of which the interaction between water vapor and T_s is the best understood and that between clouds and T_s the least understood.

The concept of radiative–convective equilibrium in a one-dimensional model enables us to formulate the climate problem in terms of forcing and feedback. The fundamental climate-forcing term is the radiative flux at the tropopause. We will describe later the feedbacks that govern the response of the climate to radiative forcing.

Radiative–convective–dynamic interactions

Including interactions between radiation, convection and planetary-scale dynamics yields two-dimensional climate models. The radiation energy is not balanced at each latitude. Regions at low latitudes receive more solar energy than do the polar regions. Sea ice and snow cover at high latitudes steepen this gradient. Such surfaces reflect much more sunlight than does the darker, open water in low- and midlatitude oceans. The tropical energy surplus and the polar deficit give rise to a strong pole-to-equator temperature gradient. The long-wave emission is much more uniform, but it does not compensate for the excess solar heating in the tropics. Thus there is a net radiative heating at low latitudes, accompanied by net cooling at high latitudes (see figure 3).

The imbalance in heating and cooling acts as the fundamental energy source for the atmospheric and ocean circulations. They must transport the excess heat from the equator toward the poles. The process is extremely complex. The net radiative heating in the tropics manifests itself in the atmosphere as latent heat released within deep cumulonimbus clouds. The heat release drives the tropical Hadley cell (see figure 4). Near the surface the flow toward the equator carries the moisture evaporated from the subtropical oceans and deposits it as tropical rain. At the surface the net solar and long-wave fluxes provide the energy required to compensate for the evaporative cooling of the oceans. The Coriolis force on the poleward motion of the Hadley cell leads to strong west-to-east winds having speeds of 20–50 m/sec in the lower 10–15 km of the atmosphere. Strong westerlies and mountain barriers give rise to dynamical instabilities that break the mean west-to-east motion into eddies, particularly at midlatitudes. Furthermore, the atmosphere does not transport all the heat: Oceans carry some through wind-driven and thermohaline circulation. (Thermohaline circulation results from the density variations in the oceanic fluid due to the combined effects of temperature and salinity.)

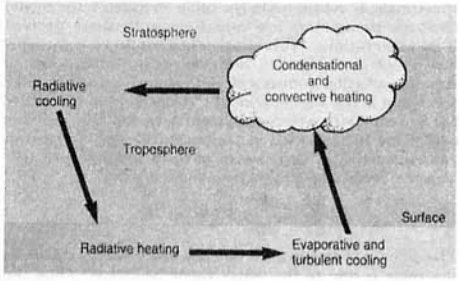

Radiative–convective interactions between the surface and the atmosphere. **Figure 2**

Climate feedback from models and satellite observations

	Climate models ($W/m^2/K$)	Satellite studies ($W/m^2/K$)
Infrared feedback (dF/dT)	1.3–2.3	1.6–2.2
Snow or ice albedo feedback $(S_0/4)(d\alpha/dT)$	−(0.3–0.6)	−0.4

Adapted from ref. 6.

More quantitatively, the divergence of heat flow in the atmosphere and oceans balances the net radiative heating H. Direct estimates of the oceanic heat transport have large uncertainties because of severe spatial sampling problems. Radiation budget measurements of H and atmospheric circulation measurements determine two of the three terms in the balance equation. Thus the oceanic heat transport is the difference between these two observations. The principal finding[4] is that in the Northern Hemisphere the oceans transport 40% of the required total heat transport. The numerical values are not yet definitive, however, because of the possibility of sampling errors in both H and atmospheric transport.

So far we have restricted our attention to the troposphere. The stratosphere is an important and integral part of the climate system as well. Radiative, dynamical and photochemical processes (see figure 4) couple it to the lower atmosphere. Absorption of solar ultraviolet radiation is a major energy source for the middle and upper stratosphere. For the lower stratosphere ozone absorption of infrared radiation at wavelengths of 9–11 μm is a significant heat source. The O_3 radiative heating rate increases with altitude and is sufficiently large to explain the observed thermal inversion in the stratosphere. The major energy sink is emission of radiation by CO_2 in the 15 μm region. Globally the solar and infrared heating by O_3 is largely balanced by the CO_2 emission, which maintains the global stratosphere in radiative equilibrium.

The O_3 radiative heating also plays an important role in governing latitudinal gradients in temperature and the circulation of the stratosphere. In winter, radiative heating is maximal in the tropics and zero near the pole tilted away from the Sun. This creates a strong temperature gradient and a correspondingly strong west-to-east jet. Countering this effect is one arising from a mechanical energy source set up by tropospheric eddies. Their energy propagates vertically and poleward into the stratosphere to heat the stratosphere near the poles and thereby reduce the equator-to-pole temperature gradient. Thus the eddies act to oppose the radiatively driven temperature gradient and circulation. For reasons not yet understood, the Antarctic stratospheric circulation is driven more radiatively than is the Arctic. As a result, the lower stratosphere of the Antarctic is significantly colder than the Arctic stratosphere and the west-to-east jet is significantly stronger. This cold and the strong jet explain the severity of the ozone hole in the Antarctic. (See the news story in PHYSICS TODAY, July 1988, page 17; also August, page 21.)

Photochemical processes in the middle and upper stratosphere (see figure 4) produce ozone that is transported poleward and downward by winds. The ozone absorbs

sunlight, and the result is a strong effect on the temperature gradients in the stratosphere.

Inadequate understanding of the strong coupling of radiation, dynamics and chemistry in the stratosphere is a major source of uncertainty in recent model projections of ozone change.

Radiation budget and climate change

Human activities alter the radiation budget. This is the central fact behind the current debate over the greenhouse effect (see the box on pages 28 and 29). As is customary, we discuss the climate change problem for the change produced by doubling the atmospheric CO_2 concentration.[5]

If we could immobilize the atmosphere and suddenly double its CO_2 concentration, the long-wave flux F would decrease by about 4 W/m^2 at the tropopause. This decrease is easy to explain. Recall from our earlier discussion that an absorbing gas decreases F because the atmosphere is colder than the surface. Thus increasing the CO_2 concentration decreases the energy loss from the troposphere to space so that the heating increases by 4 W/m^2. According to our zero-dimensional climate model, the global situation will restore the radiation energy balance. In other words, the climate system will force H to zero. The planet's surface and troposphere could warm up until it radiates to space the excess 4 W/m^2. The increase in F effected by a higher temperature balances the decrease in F caused by the increase in CO_2 concentration.

The discussions here ignore the stratosphere, which in fact will cool because of the increased CO_2 infrared emission. If the infrared emission were only a function of T and of CO_2 concentration, the total change in H would be a sum of an initial forcing term and a direct response term:

$$\Delta H = \frac{\partial F}{\partial [CO_2]} \Delta [CO_2] + \frac{\partial F}{\partial T} \Delta T$$

Initially ΔT is zero. So ΔH equals the initial forcing of F (by a change in CO_2 concentration). The climate system's tendency to equilibrium again drives ΔH to zero. Then the resulting temperature change (in the troposphere or at the surface) is

$$\Delta T = -\frac{\partial F/\partial [CO_2]}{\partial F/\partial T} \Delta [CO_2]$$

The rate at which the emission increases with increasing T governs the temperature change.

Now let us include a well-known feedback in the above thought experiment. The emission depends upon water vapor as well as carbon dioxide. As the Earth's surface warms, water evaporates more rapidly from the surface. To keep the process near equilibrium, more water must condense. However, the net result is increased water vapor in the atmosphere. This vapor will further decrease F—and increase heating. For these simple climate models, we usually assume that humidity is only a function of temperature. The energy balance equation changes accordingly to become a sum of three terms—initial forcing, direct response and indirect response:

$$\Delta H = \frac{\partial F}{\partial [CO_2]} \Delta [CO_2] + \frac{\partial F}{\partial T} \Delta T + \frac{\partial F}{\partial [H_2O]} \frac{\partial [H_2O]}{\partial T} \Delta T$$

When the system reaches equilibrium, the radiation balance perturbation vanishes (that is, $\Delta H = 0$). The final temperature change for water vapor feedback is

$$\Delta T = -\frac{(\partial F/\partial [CO_2]) \Delta [CO_2]}{\partial F/\partial T + (\partial F/\partial [H_2O])(\partial [H_2O]/\partial T)} = \frac{\Delta Q}{\lambda}$$

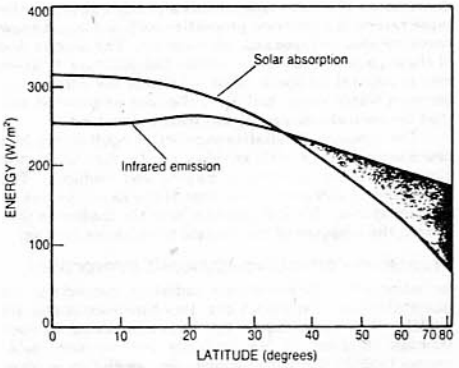

Annual zonal mean estimates of absorbed solar radiation and outgoing long-wave flux (infrared emission) obtained by satellites. Net heating (yellow) takes place at low latitudes; net cooling (blue), at higher latitudes. Equal-area projection is shown. (Adapted from ref. 10.) **Figure 3**

The numerator ΔQ is the forcing term. The denominator λ is the feedback parameter.

With a warmer atmosphere, the albedo of the planet might change. For example, the ice caps could melt or clouds could change. In other words, the climate processes would produce other feedbacks that would modify the response of the system to the initial forcing. For a change in albedo, we would call this an albedo feedback. A general expression that takes this feedback into account is

$$\lambda = \left(\frac{dF}{dT}\right) + \frac{S_0}{4}\left(\frac{d\alpha}{dT}\right)$$

Current three-dimensional climate models yield global warming by amounts in the range of 3–4.5 K. For a doubling of CO_2, the model estimate of ΔQ is about 4 W/m^2. Thus, the theoretical value of λ lies in the range 0.9–1.5 W/m^2/K. There have been many empirical estimates[6] of λ from satellite measurements of Earth's radiation budget. In general, these studies use the latitudinal and seasonal changes in the observed F, α and T to estimate λ. As shown in the table on page 24, the model feedback parameters are consistent with those derived from observations. This consistency would be a satisfactory proof of the model, however, only if the seasonal climate variation mimics a climate change caused by CO_2.

What is the significance of the numbers in the table? Let us begin with a climate system devoid of all feedbacks except for the increase in temperature. An increase in emission with an increase in surface temperature is a negative feedback. In this case, models yield[6]

$$\frac{dF}{dT} = \frac{\partial F}{\partial T} \simeq 3.3 \text{ W/m}^2\text{/K}.$$

The difference between 3.3 and the lower values shown in the table is due to the water-vapor feedback. Thus the water-vapor–temperature coupling is a positive feedback. The albedo feedback also is positive because an increase in T causes a melting of sea ice and snow cover. The decrease in the area of ice and snow lowers the albedo and thereby

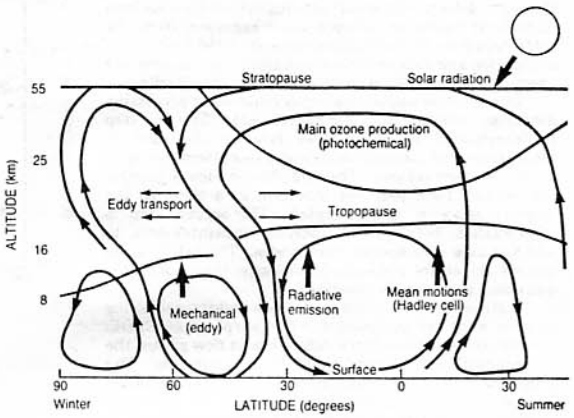

Radiative–dynamical–chemical coupling between the troposphere and stratosphere. The tropopause, which is the boundary between the troposphere and stratosphere, extends from about 8 km near the poles to as high as 17 km at low latitudes. It shifts abruptly around the latitude of the jet stream. The mean meridional circulation has been adapted from a global circulation model simulation carried out by Syukuro Manabe and Jerry Mahlman[11] of Princeton University's geophysical fluid dynamics laboratory. **Figure 4**

increases the absorbed sunlight. The whole process amplifies the surface warming.

Thus radiative interactions govern both climate forcing and the response of the climate to the forcing. It is obvious that observations of the radiation budget are important for testing theories of climate change.

Outstanding problems

The fundamental limitation of the models described above is that they lack explicit formulations for the interaction between the distribution of sources and sinks of diabatic energy (radiation and latent heat) and the dynamics of the atmosphere and oceans. Because of the limitations of simple models, a class of three-dimensional models known as general circulation models is becoming a basic tool for studying climate and climate change.

The GCMs were developed initially for forecasting weather, but are now being modified to address climate problems. The most significant modification involves the treatment of physical processes (for example, radiation, sea-ice formation and processes involving soil hydrology and vegetation) that were either ignored altogether or treated very crudely. Such models lead to significant insights into the causes of important climatological phenomena, such as the role of mountains and land–ocean asymmetries in the amplitudes and phases of planetary-scale stationary and transient waves (weather disturbances); the location and seasonal variation of the jet streams; and monsoon circulation, to name a few.

Attention is now shifting toward climate changes on time scales of decades or longer, and challenging problems such as cloud–radiation feedback (described later) and ocean–atmosphere interactions have emerged as major issues. We need an observational base of sufficient accuracy to allow us to develop and constrain our three-dimensional models. For example, we need to know how the absorption of solar radiation by the oceans, the sea ice, the tropical forests and the deserts (among other geographical features) vary with the zenith angle of the Sun and with the seasons in order to model their effects. The required observation is the clear-sky albedo of the planet (see the cover of this issue). Next, we need to know how clouds modulate the solar absorption of the various regions of the world. The required observation here is the cloud-radiative forcing (to be defined later). It is the desire for such detailed insights that motivated the ERBE studies.

ERBE has several unique features. First, the three satellites sample the Earth at different local times to minimize time sampling errors and systematic biases, which were present in earlier measurements. Second, ERBE's preflight and on-board calibrations significantly improve the accuracy and precision of the measured radiation. Third, ERBE has treated data processing much more rigorously than previous missions have.

Measurement challenges

The fundamental inference from the model studies is that climate should be extremely sensitive to small variations in radiative forcing. For example, a 1% increase in the solar irradiance will increase the absorbed solar radiation by 2.4 W/m^2. According to the λ values from GCMs, this increase would lead to a 1.6–2.6-K warming of the globe.

These sensitivities pose very stringent accuracy requirements on observations. Thus the measurement of the radiation budget has been a story of increasingly sophisticated instruments and increasingly rigorous data processing. The ERBE detectors include active-cavity radiometers and thermistor bolometers. Both types of detectors use heat to measure radiant energy. If the detectors are to be accurate, the data reduction must quantitatively relate absorbed radiation to detected heat.

As an example, consider an ideal cavity designed to accept radiation from the Earth or the Sun. This electrically heated cavity is attached to a massive heat sink, which operates at a constant temperature. The energy balance of the cavity requires that the conduction heat loss from the cavity to the heat sink be the sum of two terms, electrical heating and absorbed radiation:

$$K(T_{\text{cavity}} - T_{\text{heat sink}}) = \frac{V^2}{R} + A(1-\alpha)S_0$$

The term on the left-hand side expresses the conductive heat loss from the cavity to the heat sink. K is the heat conductivity between these two masses. Because the thermostat maintains $T_{\text{cavity}} - T_{\text{heat sink}}$ at a constant value, this heat loss is constant. Measurement of the heater voltage V determines the electrical heat released in the cavity. The heater resistance R comes from preflight measurements. The radiative power into the cavity enters through an aperture of area A, with a fraction α being reflected.

Instruments to detect radiant energy become complicated because they need to maintain heat flows. On ERBE

the cavity detectors have surrounding field-of-view limiters to prevent confusion between stray radiation from the satellite or from the Sun and radiation from the Earth. The calibration and data reduction processes must remove the effect of possible heat exchanges with the surroundings.

Quantitative understanding is required in processing data from radiation budget measurements. The first step is "inversion," which involves relating the satellite measurement of radiance to the energy loss from the top of an atmospheric column. The satellite can view a particular location from only one direction at a time, so the angular space is undersampled. The second step is interpolation between the satellite measurements to average data over specific time scales. The satellites do not see the entire globe simultaneously; thus, both time and space are sparsely sampled.

Instruments, inversion techniques and the averaging process were all advanced for the purposes of ERBE. Mathematical models of the detector heat flow guided the development and calibration of the instruments. The precursor measurements of Earth's radiation budget taken by the Nimbus-7 satellite provided data for empirical models of angular dependence. As a further aid to accurate data reduction, the angular models classify areas of the Earth into various categories of cloudiness. The ERBE time averaging took into account the detailed dependence of the albedo on solar position. For the first time, the averaging also included the diurnal variation of emission.

Where are we now with respect to producing an accurate measure of the Earth's radiation budget? First, for the instantaneous irradiance, we expect uncertainties of about 1% for long-wave and 2–3% for shortwave-radiation from the consistency of the three spectrally overlapping scanner channels. Second, for instantaneous fluxes from 2.5°×2.5° (roughly 300 km×300 km) geographic regions, ERBS and NOAA-9 intercomparisons offer observational uncertainty estimates of ± 5 W/m^2 in the long-wave and ± 15 W/m^2 in the shortwave. Third, on a monthly average, regional basis, the uncertainties in the scanner data are about ± 5 W/m^2 for shortwave and ± 5 W/m^2 for long-wave. Simulations with geostationary operational environmental satellite data provide this estimate. Fourth, the uncertainty in global, annual average net radiation is probably about ± 5 W/m^2 as estimated from the imbalance obtained using scanner data over four months. A definitive error analysis is under way.

The battle for accuracy is far from won. However, the improvements are impressive enough that understanding some of the climate problems is now within our grasp.

Solar irradiance and its variability

Changes in the solar "constant" constitute the primary external forcing of the climate system. The most apparent phenomenon that could cause the solar output to vary is sunspots. These are small portions of the solar disk with lower emission that appear black against the brilliant background of the solar disk. During the sunspot minimum, there may be no sunspots at all. During the sunspot maximum, spots may cover 1–2% of the disk. Thus if the spots emitted no energy, the solar irradiance might vary by 10–20 W/m^2. However, the spot temperatures are only 10–20% lower than the usual temperatures of the disk. This means that the actual modulation[7] of the solar irradiance by sunspots is probably 0.1–0.2%. Until spaceborne solar irradiance monitors began observing in 1979, the actual modulation was not measurable.

Detailed investigations have shown that the solar irradiance is also perturbed by bright areas known as faculae, which surround the spots. They cover a larger area than do the spots and contrast less with the disk.

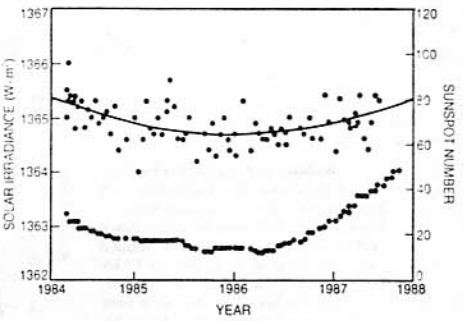

Solar constant as a function of time, derived from the solar monitor on the Earth Radiation Budget Satellite. The blue curve represents a second-order polynomial fit to the solar constant values; the red dots represent smoothed (12-month running mean) sunspot numbers. (Data from ref. 7.) **Figure 5**

Evidently, after sunspots develop, faculae increase and raise the solar irradiance. The solar irradiance is indeed lowest at the sunspot minimum, when the radiant contribution by faculae is also a minimum. Figure 5 shows this behavior over three years of ERBE solar observations. Before the sunspot minimum in 1986, the observed solar irradiance decreased at a rate of 0.02%/year. After the minimum, it increased at the same rate. All three of the solar irradiance experiments have measured similar decreases and increases.

The observational record for sunspots extends far enough into the past that it is a prime candidate for empirical modeling. The time series of facular observations is not as long. However, researchers are developing empirical models of the correlations between sunspots and faculae. These would allow us to investigate the correlation between climate and the Sun.

Diurnal variations in Earth's radiation fields

Poor diurnal sampling was one of the principal sources of uncertainty in earlier radiation budget measurements. Most of the Earth radiation budget instruments before ERBE flew on single, Sun-synchronous satellites. Satellites in these orbits sampled the Earth at only one local time during the day and once at night. ERBE is the first multiple-satellite system to provide diurnal sampling capability for global radiation budget studies.[8] Two NOAA satellites are in Sun-synchronous orbits, and NASA's Earth Radiation Budget Satellite is in a mid-inclined orbit. ERBS's orbit precesses through all local hours at the equator in 36 days (when one counts both ascending and descending nodes). This 56° inclination orbit provides diurnal coverage over the tropics. It also provides coverage of the midlatitudes, where the maximum diurnal range of long-wave radiation occurs. The two NOAA satellites supplement this diurnal coverage at low latitudes. They also provide the necessary coverage over the polar regions.

In addition to minimizing sampling errors, diurnal cycle observations provide critical insights into climate feedback processes involving the land surface, meteorology and solar heating, because several types of variability

Human Activities, Greenhouse Effect and Climate Change

The pertubations to the planetary radiative heating caused by human activities have begun to rival or exceed those due to naturally induced changes.

Since the dawn of the industrial era, human activities have been altering the chemical composition of the atmosphere.[12] The increase in several radiatively active gases in the atmosphere, which apparently began in the 19th century and continues today at alarming rates, is particularly important. These gases include CO_2, CH_4, $CFCl_3$, CF_2Cl_2 (and many other chlorofluorocarbons), N_2O and O_3. Of these, the most important for the greenhouse effect, according to current perception, are CO_2, CH_4 and CFCs. From 1975 to 1985, CFCs doubled, CH_4 increased by 9–10% and CO_2 increased by 4.5–5%. During the last 100–200 years CO_2 increased by 25%, while CH_4 concentration seems to have doubled. The increase in radiatively active gases warms the climate through a chain of forcing and feedback mechanisms. These gases absorb and emit photons at wavelengths of 7–20 μm. Thus the internal motions of the atmosphere's molecules receive energy from photons emitted by the Earth's surface. Collisions between molecules change this internal energy into the kinetic energy of the molecules themselves, that is, into heat. The net effect of this process is to increase the radiative heating of the planet by reducing the radiation energy emitted to space (see main text). The magnitude of the increase is given in the table on page 29.

The H_2O greenhouse feedback and the ice-albedo feedback amplify the surface warming. According to current model predictions, the anthropogenic greenhouse forcing from 1850 to 1985 (see the table on page 29) has committed the planet to a global surface warming in the range 0.8–2.4 K; even if the trace gas concentrations were to stop increasing today, the planet will still warm by 0.8–2.4 K. (The three-fold range is the currently perceived uncertainty in model predictions.) If, on the other hand, the currently observed growth rates continue unabated, the committed warming can double within the next 50 years. Not all of the committed warming will be realized immediately, since the enormous heat capacity of the oceans will delay the warming. Turbulent mixing of the added heat within the top 50–200 meters of the ocean (the so-called mixed layer) and the large-scale lateral and vertical mixing by the circulation in the deeper layers can delay the warming for decades to longer than a century. This important role of the oceans is poorly understood. Because of this lag, the transient warming is between a third and a half of the committed warming. The table on this page summarizes some model predictions.

The global warming is accompanied by substantial changes in other climate parameters and in regional climate. These changes include the poleward retreat of sea ice, poleward amplification of the warming, enhanced global precipitation, increased sea level, drying of midcontinents at midlatitudes, and increased intensity of tropical storms. The magnitudes of the regional effects are highly model dependent. Even the sign of some of the effects, such as drying of the midcontinents, is model dependent.

Then is the greenhouse warming a proven fact or still an untested theory? Satellite observations of the long-wave emission and albedo certainly confirm the infrared trapping effect of the present atmosphere and the resulting surface warming effect (see text). We are reasonably certain that the planet would be significantly colder without the radiatively active gases in the present atmosphere. By deduction, then, an increase in the radiatively active gases should heat the planet; this also seems certain. The magnitudes of the warming and the accompanying regional changes, however, are governed by numerous feedbacks, and only one of these, the H_2O temperature feedback, is well understood. Confidence in the model predictions would be significantly greater were it not for our lack of understanding of two important feedbacks: cloud-radiative interactions and ocean–atmosphere interactions. To illustrate the nature of the difficulty, let us consider the cloud-radiative feedback.

The global mean long-wave and shortwave cloud forcing are both larger than the trace gas forcing of about 2.2 W/m^2 by a factor of 15–20. The shortwave effect forces the system toward a cooler climate, while the long-wave effect forces it toward a warmer climate. In the present climate, the balance has tilted toward shortwave forcing—that is, net cooling. It is not understood how the balance will shift in an atmosphere abundant with greenhouse gases. Current GCMs suggest that the balance of cloud forcing is shifting toward heating (that is, less net cooling) as the planet warms.[14,15]

To examine the regional feedbacks, consider the severe summer drying of midcontinents as predicted by one of the general circulation models.[15] During July 1985, the Earth Radiation Budget Experiment data show, the shortwave forcing in the mid-North American continent was about -50 W/m^2; that is, the reflection of solar radiation by clouds reduced the absorbed solar energy by 50 W/m^2. Suppose the clouds disappeared in certain regions subjected to drying. The lack of shortwave cloud forcing would provide an additional radiative heating of 50 W/m^2, significantly larger than the initial 2-W/m^2 radiative forcing of trace gases. The main point is that regional changes or shifts in clouds in response to trace gas heating can cause changes

Predicted transient changes of world temperatures due to trace gas effects

Altitude	Latitude	Season	Temperature change[1] (K)	
			1850–1985	1960–2010
Surface–air interface	Global mean	Annual	+ (0.5–1.0)	+ 1.0
Surface–air interface	Sea-ice margins (50°–70°)	Winter	+ (1.5–3.0)	+ (1.0–3.0)
Surface–air interface	Polar continents	Spring	+ (0.8–1.5)	+ (1.0–2.0)
Stratosphere (30 mb)	Global	Annual	− 1 (cooling)	—
Stratosphere (1 mb)	Global	Annual	− 6 (cooling)	—

[1]Data for 1850–1985 based on ref. 13. Values for 1960–2010 estimated from ref. 14.

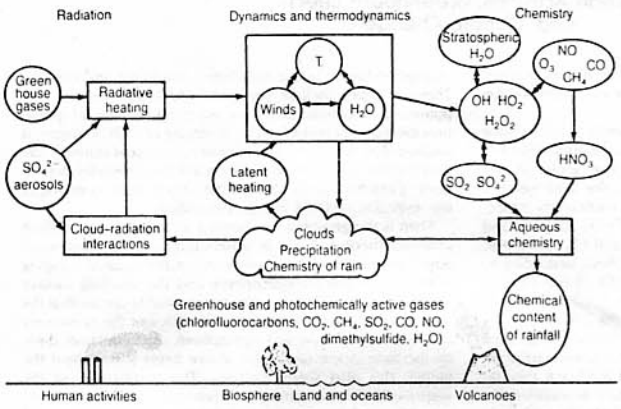

Coupling between climate and atmospheric chemistry. (Adapted from unpublished work[19] by Paul Crutzen, Leo Donner, Ramanathan and Ramesh Srivastava.)

in regional radiative heating patterns that are an order of magnitude larger than the radiative heating due to the increase in trace gases.

Comparison with other planets provides a useful perspective. Consider Venus. At the top of its atmosphere, Venus receives almost twice as much solar radiation as does the Earth (S_0 for Venus is 2620 W/m²). However, Venus is completely cloud covered with an albedo[16] of 80%, compared with 30% for the Earth. Hence Venus absorbs only 130 W/m², that is, roughly 55% as much as the Earth (see text). Despite absorbing significantly less solar energy, Venus has a much hotter surface than the Earth. Its surface temperature, 750 K, is maintained by the greenhouse effect of CO_2, clouds and water vapor.[17] The magnitude of the total Cytherean greenhouse effect can be estimated easily. At a surface temperature of 750 K, Venus emits about 17 900 W/m². Only about 130 W/m² escapes to space, because this is the required emission to balance the absorbed solar energy. Thus the atmosphere traps about 17 770 W/m², nearly two orders of magnitude greater than either the solar absorption or the Earth's greenhouse effect.

The above comparison suggests that there is no conceivable saturation point for the atmospheric greenhouse effect; it is limited only by the concentration of gases in the atmosphere. Note also that on Venus clouds have been unable to offset the greenhouse effect to any significant extent.

An important limitation of the models and the arguments given above is that they ignore the role of the biosphere. A recent study[18] suggests the existence of a negative cloud feedback involving marine organisms. The nuclei around which vapor condenses to form boundary-layer clouds are predominantly sulfate aerosols. The new study shows that the sulfate aerosols are formed from dimethylsulfide emitted by phytoplankton. The study speculates that an increase in ocean temperatures can lead to increased emission of DMS, which, in turn, will result in more sulfate aerosols. The increase in the number of cloud drops (due to the increase in aerosol concentration) will scatter more sunlight; that is, the shortwave cloud forcing will become more negative. Thus, the net cloud forcing effect will tend toward more cooling and offset the greenhouse effect.

In summary, as we probe more deeply into the climate problem, it is becoming increasingly apparent that models of climate, whether they are pedagogical or three-dimensional numerical models, should account not only for the interactions among the physics, the chemistry and the dynamics but also for the interactions of the biosphere with the rest of the climate system.[12] In addition to perturbing Earth's radiation balance, gases emitted by human activities perturb the chemical balance—especially the chemistry of ozone, hydroxyl radicals, sulfur oxides and nitrogen oxides (see the figure above). Biogenic and anthropogenic emissions are the basic sources of many reactive gases (for example, CO, CH_4, NO and DMS). These gases are oxidized by reaction with the hydroxyl radical (OH), which in turn is derived from the reaction of H_2O with an oxygen atom. The atmospheric concentration of H_2O is governed by the distribution of temperature, winds and surface evaporation. Several of the reaction products (for example, HCl, H_2SO_4 and HNO_3) are soluble and are removed by cloud drops and raindrops. The atmospheric chemistry in turn determines the vertical distribution of some of the greenhouse gases (CH_4, O_3 and NO_2) and the concentrations of condensation nuclei for clouds. These gases and clouds modulate the radiative heating of the planet, which, of course, drives the general circulation (see also the text). No current model accounts for these interactions, and we are perhaps decades away from developing one that does. In the meantime, we face the unenviable task of judging the seriousness of the anthropogenic effect with a very limited comprehension of the climate system. The question, however, is not, Is the problem serious? but, At what concentration levels will the trace gases trigger an unprecedented climate change?

Anthropogenic greenhouse forcing (W/m²)

	1850–1985	1975–1985
CO_2 (only)	1.3	0.24
All trace gases	2.2	0.45

Adapted from ref. 13.

are synchronized with the Sun. The global distribution of the diurnal range of long-wave radiation for July 1985 (see figure 6) reveals patterns that can be related not only to the heating and cooling of the surface but also to diurnal changes in cloud cover and in the vertical structure of clouds.

The largest diurnal variation of long-wave radiation (about 60 W/m^2) occurs over deserts (the Sahara, Saudi Arabia, the Gobi, the Great Sandy, the Atacama, the southwestern US and Kalahari). In fact, with a few exceptions, the diurnal range is closely correlated with the aridity and vegetation cover of the soil. The drier the soil and the sparser the vegetation, the more the Sun heats the ground (instead of evaporating moisture) and so enhances both the amplitude of the diurnal temperature variation and the long-wave emission. The major exceptions are the vegetated regions of Central America, and the northern Amazon and Congo basins, which have diurnal variations as large as 40 W/m^2. These regions experience intense convective cloud activity, and the cloud shield undergoes a strong diurnal cycle. Because ocean surface temperatures are relatively constant, diurnal variations of long-wave flux over the oceans are generally small (less than 10 W/m^2) and are due primarily to changes in clouds. An intriguing possibility raised by the global pattern shown in figure 6 is that regional scale shifts in soil hydrology (due, say, to deforestation) can be detected by monitoring the diurnal range of long-wave flux.

Clouds and climate

Do clouds heat or cool the planet? This question has perplexed many working on the theory and modeling of climate. An unambiguous theoretical estimate is still lacking.

When atmospheric water vapor condenses to a liquid or a solid, it scatters ultraviolet and visible radiation significantly compared with cloudless skies. The scattering is both forward to the ground and backward to space. An individual droplet scatters 85% of the incident energy in the forward direction. A cloud of drops, however, can scatter 75% or more of the energy backward. The resulting enhancement in the surface-atmosphere albedo reduces the solar radiation absorbed by the atmospheric column.

Clouds also significantly enhance the long-wave opacity of the atmosphere. Like the gaseous absorption, this reduces the radiation emitted to space. Thus, while the greenhouse effect of clouds warms the planet, the albedo effect cools it. The problem is further complicated by the significant dependence of cloud radiation on cloud microphysics. These properties include the density of liquid water and droplet size distribution, both of which vary significantly from one cloud to another. As a result the albedo and the greenhouse effects are subject to significant variability.

Cloud-radiative forcing: a simple approach

It is a challenge to measure the two competing effects of clouds on the radiation budget. The major problem is that cloud structures vary in scale from meters to thousands of kilometers. This means that many of the "satellite pixels" image mixtures of clear and overcast regions (or "scenes"). As a result it is nearly impossible to unscramble the radiances to produce an overcast radiance.

ERBE has found a rather simple approach to this problem,[9] one that is quite successful in obtaining the net radiative effect of clouds on climate. It starts with the observation that the spatial variability is considerably smaller in clear-sky fluxes than in mixed-scene fluxes. The clear-sky flux is also an extremal value: The "hottest" long-wave radiances and the "darkest" shortwave radiances come from clear skies. Therefore clear skies are easier to identify than mixed skies are. Spatial homogeneity also makes it easier to estimate what the clear-sky fluxes would have been if the clouds were not present.

Let us make this discussion more quantitative by considering a region partially covered by clouds. The region can be the entire planet, an entire latitude belt or a specific region of the globe. Let f be the fraction that is covered by clouds. We define F as the average flux emitted to space by this region from the cloud condition *in toto*. F_c is the flux from the clear-sky portion. F_0 is the flux from the overcast sky. We can then write

$$F = (1 - f)F_c + fF_0$$

How can we observe the clouds' influence on F and, ultimately, on the net heating H? We can rewrite F as

$$F = F_c - f(F_c - F_0) = F_c - C_{LW}$$

For a region with multilayer clouds, C_{LW} is redefined as

$$C_{LW} = \sum_i f_i(F_i - F_{0,i})$$

where the summation extends over i different cloud layers.

To find C_{LW} from observations of cloudy regions, we have to identify the individual overcast areas and their radiative properties. As we discussed earlier, this has many difficulties. However, C_{LW} can also be obtained

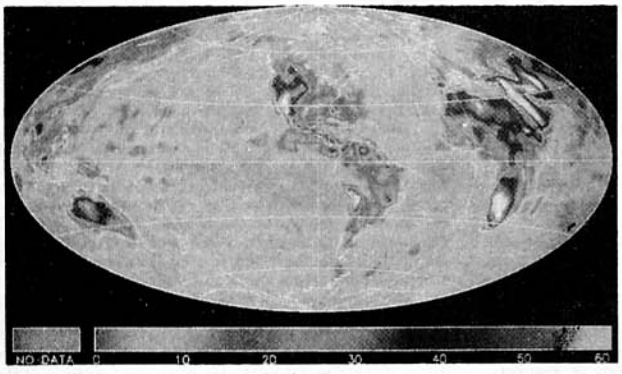

Diurnal range of long-wave flux (in W/m^2) as seen by ERBE for July 1985. (See ref. 8 for additional details.) **Figure 6**

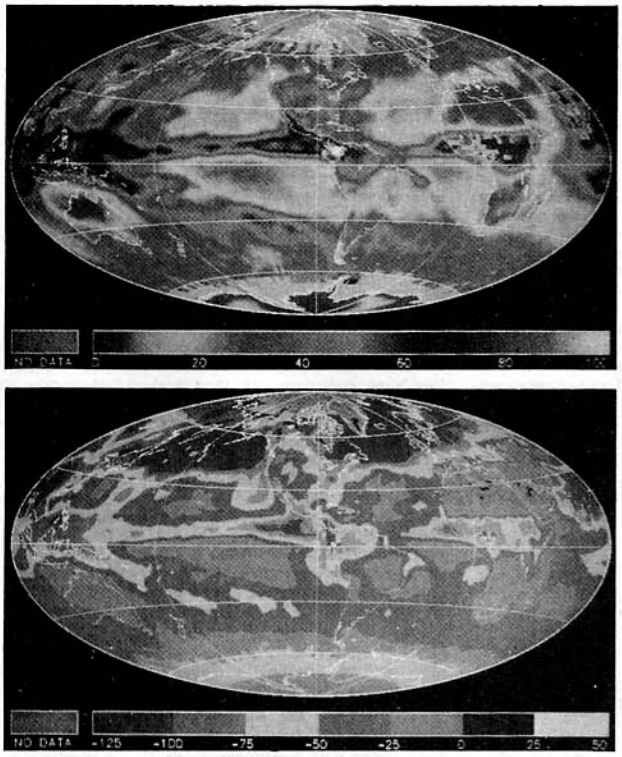

Cloud-radiative forcing (in W/m²). Monthly averages derived from ERBE for July 1985 are depicted for long-wave (top) and shortwave forcing (bottom). Long-wave cloud forcing is the reduction by clouds in the long-wave radiation that is emitted to space; hence it is the greenhouse effect of clouds. Clouds reduce emission to space because at their bases they absorb radiation emitted by the warmer surface and at their tops they emit to space at colder temperatures. Deep cirrus clouds such as the monsoon cloud systems over the Indian Ocean and Indonesia and the jet-stream cirrus clouds at midlatitudes give a large greenhouse effect. Because clouds reflect more shortwave solar radiation than the adjacent clear skies, the shortwave forcing is negative—a cooling effect. Surprisingly, the magnitude of the cooling is as large as the long-wave forcing over the tropical cirrus systems, and is even larger over the mid- and high-latitude oceans. The net cloud-radiative forcing (shown in the bottom image on the cover) is the sum of long-wave and shortwave cloud forcing. The averages range from −(100–140) W/m² (dark blue) to 10–40 W/m² (red). The net effect is largely negative; hence clouds have a cooling effect on the planet. The strongest cooling is caused by persistent stratus and storm-track clouds over mid- and high-latitude Atlantic and Pacific oceans. **Figure 7**

from the equation for F:

$$C_{\mathrm{LW}} = F_c - F$$

Thus obtaining the cloud effects on climate reduces to obtaining the clear-sky flux, a considerably simpler problem. For reasons that will become obvious later, we refer to C_{LW} as the long-wave forcing.

Likewise, we can define C_{SW} as the difference in the reflected solar flux between clear and cloudy skies. The net cloud-radiative forcing, C, is then the sum of the long-wave and the shortwave cloud forcing.

In the long-wave, cloudy-sky fluxes F, are usually lower than the clear-sky fluxes F_c, giving $C_{\mathrm{LW}} > 0$. In other words, clouds produce an additional greenhouse effect that forces the surface temperature to be higher than it would be otherwise. In the shortwave, cloudy fluxes are usually higher, so $C_{\mathrm{SW}} < 0$. In this case, the clouds force the climate system to be cooler. Clearly, "forcing" is an appropriate name. Note that if clouds were absent, f would be zero and so would C. (The total flux in the absence of clouds is the clear-sky flux $F = F_c$.)

An exciting outcome of this approach is that it produces a global estimate of the clear-sky albedo of the planet. The albedo distribution reveals" the oceans to be the darkest region of the globe (shown in the top panel of the cover, which adopts the following color scheme for albedo: blue is 6–13%, green is 13–20%, yellow is 20–30%, red is 30–45%, white is 45–80%). Albedo values range from 6–10% in low latitudes to 15–20% in the polar oceans. The brightest regions of the globe are, of course, the snow-covered Arctic and Antarctic. Next in brightness are the deserts, with the Sahara reflecting as much as 40% of the incident solar radiation. The other major deserts, such as those of Saudi Arabia, the Gobi and the Great Sandy, reflect about 25–35%. The darkest land surfaces are the tropical rain forests of South America and central Africa. Thus clearing of forests in the tropics should have a significant impact on the regional heat balance.

As of this writing ERBE has processed four months of data: April 1985, July 1985, October 1985 and January 1986. Figure 7 shows the long-wave and shortwave cloud forcing for July 1985. These measurements provide a global perspective that was previously lacking.

The cloud-forcing patterns mirror the major climate regimes and the organized cloud systems of the planet. For example, the peak values of the long-wave cloud forcing (figure 7, top) reveal organized convective- and cirrus-cloud systems in the tropics. These are present over the monsoon regions of the tropical Pacific and Indian Oceans, over central Africa and over the Amazon basin. At midlatitudes the cloud forcing coincides with storm tracks and jet-stream cirrus systems.

The organized pattern of time-averaged cloud forcing stands in sharp contrast to the more chaotic spatial structure within individual cloud systems. This pattern of cloud forcing is encouraging, since GCMs are quite successful in simulating the time-averaged patterns of the

large-scale circulation. With a physically realistic model of clouds, it should be possible to use our climate models to estimate their radiative effects.

In contrast to the long-wave forcing, shortwave forcing (figure 7, bottom) peaks in the midlatitudes. The shortwave forcing is as large as the long-wave forcing in the monsoons and quasistationary convective regions. In the more poleward oceans, the shortwave forcing exceeds the long-wave forcing by more than 100 W/m^2.

The net cloud-radiative forcing is shown in the bottom panel of the cover. Regions where clouds have a net cooling effect are shown as green (-10 to -30 W/m^2), light blue (-30 to -60 W/m^2), medium blue (-60 to -100 W/m^2), dark blue (-100 to -140 W/m^2); a net warming effect is indicated by red ($+10$ to $+40$ W/m^2); and the transition region between cooling and heating is indicated by yellow (-10 to $+10$ W/m^2). The gray color indicates missing data. Two intriguing features are revealed:

▷ Regions in the tropics where net cloud forcing nearly vanishes. However, clouds produce major changes in both the long-wave and shortwave fluxes. The two forcing terms nearly cancel each other within ± 10 W/m^2 (the uncertainty in the estimate). We do not understand the physical and dynamical constraints that require these systems to have such a delicate balance.

▷ Regions of large negative cloud forcing over the midlatitude and polar oceans. Clouds reduce the radiative heating in these areas by as much as 100 W/m^2. In these regions, the dominant cloud systems are storms associated with cyclones and extensive layers of stratus clouds. These systems are very sensitive to surface temperatures and temperature gradients in the troposphere. Hence these oceanic clouds can have a significant feedback effect on climate change.

Global effects

The global averaged long-wave forcing for July 1985 is 30.1 W/m^2; it is the greenhouse effect of clouds. It is larger than that resulting from a doubling of CO_2 by a factor of about 7. The CO_2 concentration in the atmosphere has to be increased by more than two orders of magnitude to produce a greenhouse effect comparable to that of the clouds. The shortwave cloud forcing for July 1985 is -46.7 W/m^2. The net cloud forcing, which is the sum of long-wave and shortwave cloud forcing, is -16.6 W/m^2. A negative cloud forcing of similar magnitude was also obtained for three other months that have been analyzed so far: April 1985, October 1985 and January 1986. Thus the ERBE results reveal that clouds have a global *cooling* effect.

The global mean cloud-radiative cooling, when averaged over all seasons, should be balanced by a corresponding global mean radiative heating under clear skies to maintain global energy balance. Without the -16 W/m^2 cloud forcing, the planet would be significantly warmer. The magnitude of the warming would depend on the model we use to convert the forcing into a temperature change, but it could be as large as 10–15 K. The long-wave cloud forcing heats the surface–atmosphere column, while the shortwave forcing cools it. In the current climate, the shortwave effect dominates. Why this is so is not at all obvious.

The atmospheric and ocean circulations govern the generation of clouds. These circulations respond to the sources and sinks of radiative and thermodynamic energy that are governed by the distribution of clouds. Hence a climate change could change the net cloud forcing, and that change could in turn feed back into the climate. The exploration of how these changes might occur is one of the central questions in climate theory today.

We can understand specific components of the feedback by studying the evolution of cloud forcing during climate changes on shorter time scales. One spectacular example is the El-Niño phenomenon. The warm sea-surface temperature anomaly in the Pacific results in a perturbation of the convective cloud system, which is accompanied by large changes in long-wave and shortwave cloud forcing. This natural experiment provides a unique opportunity to examine the link between sea-surface temperature changes and cloud-radiative forcing. Likewise, a comparison of the shortwave cloud forcing over North America during the drought year of 1988 with the forcing during the previous years would help establish the link between soil moisture, cloudiness and regional radiative heating.

We now have the necessary (but not sufficient) observational base to develop the theory of climate change. The effects of human activities, such as the increase in trace gases or the alteration of the surface albedo by deforestation, alter the clear-sky radiative heating. Hence observations of changes in clear-sky radiative forcing on time scales of a few to several decades would document the influence of human activities. Observations of long-term changes in cloud-radiative forcing would help establish the importance of cloud–climate feedback.

• • •

The principal investigators of the ERBE science team are Barkstrom, R. Cess, J. Coakley, Y. Fouquart, A. Gruber, Harrison, D. Hartmann, B. Hoskins, F. House, F. Huck, R. Kandel, M. King, A. Mecherikunnel, A. Miller, Ramanathan, E. Raschke, L. Smith, W. Smith and T. Vonder Haar. *Ramanathan was supported by a NASA ERBE grant and NSF grant ATM8700286.*

References

1. F. B. House, A. Gruber, G. E. Hunt, A. T. Mecherikunnel, Rev. Geophys. **24**, 357 (1986).
2. B. R. Barkstrom, Bull. Am. Meteorol. Soc. **65**, 1170 (1984).
3. R. D. Cess, G. L. Potter, Tellus **39A**, 460 (1987).
4. T. H. Vonder Haar, A. H. Oort, J. Phys. Oceanogr. **3**, 169 (1973).
5. M. E. Schlesinger, J. F. B. Mitchell, Rev. Geophys. **25**, 760 (1987).
6. V. Ramanathan, J. Geophys. Res. **92**, 4075 (1987).
7. R. Lee, B. R. Barkstrom, R. D. Cess, Appl. Opt. **26**, 3090 (1987).
8. E. F. Harrison, D. R. Brooks, P. Minnis, B. A. Wielicki, W. F. Staylor, G. G. Gibson, D. F. Young, F. M. Denn, ERBE Science Team, Bull. Am. Meteorol. Soc. **69**, 1144 (1988).
9. V. Ramanathan, R. D. Cess, E. F. Harrison, P. Minnis, B. R. Barkstrom, E. Ahmad, D. Hartmann, Science **243**, 57 (1989).
10. J. S. Ellis, T. H. Vonder Haar, Atmospheric Sciences Report 240, Dept. Atmos. Sci., Colorado State U., Fort Collins (1976).
11. S. Manabe, J. Mahlman, J. Atmos. Sci. **33**, 2185 (1976).
12. F. S. Rowland, I. S. A. Isaksen, eds., *The Changing Atmosphere*, Wiley, New York (1988). R. E. Dickinson, ed., *The Geophysiology of Amazonia: Vegetation and Climate Interactions*, Wiley, New York 1987); see the articles by J. E. Lovelock, p. 11; P. J. Crutzen, p. 107; R. C. Harriss, p. 163.
13. V. Ramanathan, Science **240**, 293 (1988).
14. J. Hansen, I. Fung, A. Louis, D. Rind, S. Lebedeft, R. Rudey, G. Russell, J. Geophys. Res. **93**, 9341 (1988).
15. R. T. Wetherald, S. Manabe, J. Atmos. Sci. **45**, 1397 (1988).
16. M. G. Tomasko *et al.*, J. Geophys. Res. **85**, 8187 (1980).
17. J. B. Pollack, O. B. Toon, R. Boese, J. Geophys. Res. **85**, 8223 (1980).
18. R. J. Charlson, J. E. Lovelock, M. O. Andrae, S. G. Warren, Nature **326**, 665 (1987).
19. P. J. Crutzen, L. Donner, V. Ramanathan, R. C. Srivastava, "Clouds, Chemistry and Climate," research proposal submitted to NSF (1988). ■

Extracted from PHYSICS TODAY, May 1989